

Modifications and Improvements on Iris Recognition

Artur Ferreira^{1,2}, André Lourenço^{1,2}, Bárbara Pinto¹, Jorge Tendeiro¹

¹*Instituto Superior de Engenharia de Lisboa, Lisboa, PORTUGAL*

²*Instituto de Telecomunicações, Lisboa, PORTUGAL*

Email: arturj@cc.isel.ipl.pt, alourenco@deetc.isel.ipl.pt, {24685;24277}@alunos.isel.ipl.pt

Keywords: Iris Recognition, Biometrics, Image Processing, Image Segmentation.

Abstract: Iris recognition is a well-known biometric technique. John Daugman has proposed a method for iris recognition, which is divided into four steps: segmentation, normalization, feature extraction and matching. In this paper, we evaluate, modify and extend John Daugman's method. We study the images of CASIA and UBIRIS databases to establish some modifications and extensions on Daugman's algorithm. The major modification is on the computationally demanding segmentation stage, for which we propose a template matching approach. The extensions on the algorithm address the important issue of pre-processing, that depends on the image database, being especially important when we have a non infra-red camera (e.g. a WebCam). For this typical scenario, we propose several methods for reflexion removal and pupil enhancement and isolation. The tests, carried out by our C# application on grayscale CASIA and UBIRIS images, show that our template matching based segmentation method is accurate and faster than the one proposed by Daugman. Our fast pre-processing algorithms efficiently remove reflections on images taken by non infra-red cameras.

1 INTRODUCTION

Human authentication is of central importance in modern days (Maltoni et al., 2005)(Jain et al., 2004). Instead of passwords, or magnetic cards, biometric authentication is based on physical or behavioral characteristics of humans. From the set of biological characteristics, such as face, fingerprint, iris, hand geometry, ear, signature, and voice, iris recognition is considered extremely accurate and fast. From its characteristics the fact that it is considered unique to an individual, its epigenetic pattern remains stable through life, and the pattern variability is enormous among different persons make iris very attractive for use as biometric for authentication and identification.

The problem of iris recognition attracted a lot of attention in the literature: John Daugman (Daugman, 1993), Boles (Boles, 1997), and Wildes (Wildes, 1997) were the precursors of the area. Several modifications on work of Daugman have been proposed in the last decade: (Yao et al., 2006) uses different filters;(Greco et al., 2004) applies Hidden Markov Models to choose a set of local frequencies;(Joung

et al., 2005) modifies the normalization stage; (Arvacheh, 2006) changes segmentation and normalization; (J.Huang et al., 2004) modifies segmentation.

In this paper we follow John Daugman approach (Daugman, 1993) introducing several variations on the segmentation step based on templates and focusing the tuning of the algorithm for the UBIRIS database (Proença and Alexandre, 2005)(Proença, 2007)¹. We also propose pre-processing techniques for reflexion removal, and pupil enhancement and isolation. The proposed algorithms are also evaluated on the CASIA (Chinese Academy of Sciences Institute of Automation) database².

The paper is organized as follows. Section 2 presents the steps of an iris recognition algorithm and details Daugman's approach. Section 3 describes the standard test images from CASIA and UBIRIS databases. Modifications to Daugman's method and new approaches for pre-processing are proposed in Section 4, along with a study of CASIA and UBIRIS

¹iris.di.ubi.pt/index.html

²www.sinobiometrics.com

images. Discussion of experimental results and conclusions are drawn in Sections 5 and 6, respectively.

2 IRIS RECOGNITION

The process of iris recognition is usually divided into four steps (Vatsa et al., 2004):

- segmentation - localization of iris region in a eye image, that is the inner and outer boundaries of the iris (see figure 1); can be preceded by a pre-processing stage to enhance image quality;
- normalization - create a dimensionality consistent representation of the iris region (see figure 2);
- feature extraction - extracting information that can be used to distinguished different subjects, creating a template that represents the most discriminant features of the iris; typically it uses texture information;
- matching - the feature vectors are compared using a similarity measure.

2.1 DAUGMAN'S APPROACH

Consider an intensity image $I(x, y)$, where x and y denote respectively the rows and columns of an image. The problem is to automatically find the iris and extract its characteristics.

The segmentation step of (Daugman, 1993), localizes the inner and outer boundaries of the iris with the integro-differential operator

$$\max_{r, x_0, y_0} \left| G_{\sigma}(r) * \frac{\partial}{\partial r} \oint_{r, x_0, y_0} \frac{I(x, y)}{2\pi r} \partial s \right|, \quad (1)$$

in which r represents the radius, x_0, y_0 the central pixel and $G_{\sigma}(r)$ a gaussian filter used to soften the image (with σ standard deviation). The operator formulates the problem as the search for the circle (center: x_0, y_0 and radius) where occurs a maximum change in pixel values between adjacent circles. Fixing different centers, first derivatives are computed varying the radius; its maximum corresponds to a boundary.

Figure 1 shows an eye image with red and yellow circles representing the iris and pupil boundaries, respectively. On the right is illustrated the segmented iris; note the presence of the upper eyelids.

The normalization step transforms the iris region into a normalized image, with fixed size, allowing comparisons of different iris sizes. Iris may have different sizes due to pupil dilation caused by varying levels of illumination. The rubber sheet model (Daugman, 1993), remaps each point (x, y) of the iris image,

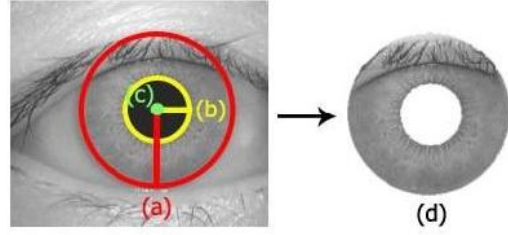


Figure 1: Segmentation Step: a) radius of the iris b) radius of the pupil c) center d) segmented iris.

into an image $I(r, \theta)$ where $r \in [0, 1]$ and $\theta \in [-\pi, \pi]$, according to

$$I(x(r, \theta), y(r, \theta)) \rightarrow I(r, \theta). \quad (2)$$

The transformation from cartesian to normalized polar coordinates, uses the mapping

$$\begin{cases} x(r, \theta) = (1-r)x_{pupil}(\theta) + rx_{iris}(\theta) \\ y(r, \theta) = (1-r)y_{pupil}(\theta) + ry_{iris}(\theta), \end{cases} \quad (3)$$

where (r, θ) are the corresponding normalized coordinates, and x_{pupil}, y_{pupil} and x_{iris}, y_{iris} the coordinates of the pupil and iris boundary along θ angle. Figure 2 presents an example of the produced normalized representation; it is possible to observe in the left image that the center of the pupil can be displaced with respect with the center of the iris. The right image represents the normalized image: on the x-axis are represented the angles (θ), and on the y-axis the radius (r). Observe that the upper eyelids are depicted on the lower right corner. Figure 3 shows the segmen-

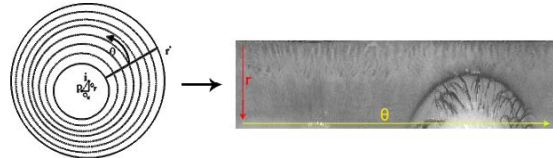


Figure 2: Normalization Step: Daugman's rubber sheet model.

tation and normalization steps for the 3 considered databases. To encode the iris pattern, 2D Gabor filters are employed

$$G(r, \theta) = e^{-i\omega_0(\theta_0 - \theta)} e^{-\frac{(r_0 - r)^2}{\alpha^2}} \cdot e^{-\frac{(\theta_0 - \theta)^2}{\beta^2}}. \quad (4)$$

These filters are considered very suitable to encode texture information and are characterized by three parameters: spacial localization x_0, y_0 , spacial frequency w_0 and orientation θ_0 , and gaussian parameters (α, β) . Figure 4 presents the individual components of the filter. The application of this filter on

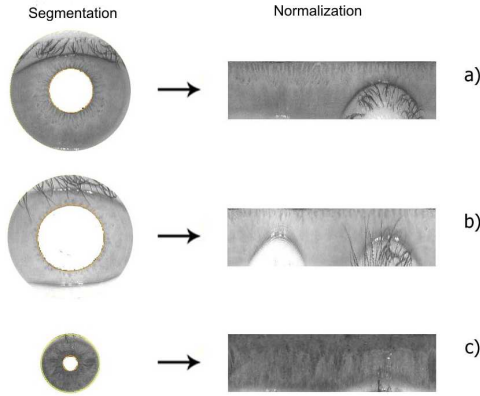


Figure 3: Segmentation and normalization steps: a) CASIAv1 b) CASIAv3 c) UBIRISv1.

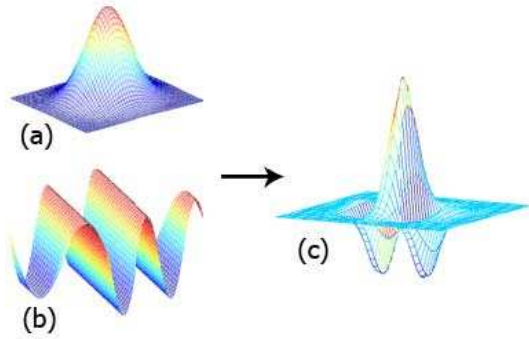


Figure 4: Feature Extraction with 2D Gabor filters: a) gaussian; b) 2D sinusoid; c) the resulting filter.

the image generates a complex image representing the relevance of the texture for a given frequency and orientation. Several filters are applied in order to analyze different texture information. This set of filters is defined by

$$GI = \int_{\rho} \int_{\phi} e^{-i\omega(\theta_0 - \phi)} e^{-\frac{(\rho_0 - \rho)^2}{\alpha^2} - \frac{(\theta_0 - \phi)^2}{\beta^2}} I(\rho, \phi) \rho d\rho d\theta \quad (5)$$

Figure 5 shows the Gabor filters considered for this purpose. The output of the filters is quantized using the real and imaginary part, $\text{Re}(GI)$ and $\text{Im}(GI)$, respectively by

$$h_{Re} = \begin{cases} 1, & \text{if } \text{Re}(GI) \geq 0 \\ 0, & \text{if } \text{Re}(GI) < 0, \end{cases} \quad (6)$$

$$h_{Im} = \begin{cases} 1, & \text{if } \text{Im}(GI) \geq 0 \\ 0, & \text{if } \text{Im}(GI) < 0. \end{cases}$$

These four levels are quantized using two bits. The so called ‘‘IrisCode’’ has 2048 bits (256 bytes), computed for each template, corresponding to the quantization of the output of the filters for different orientations and frequencies (1024 combinations).

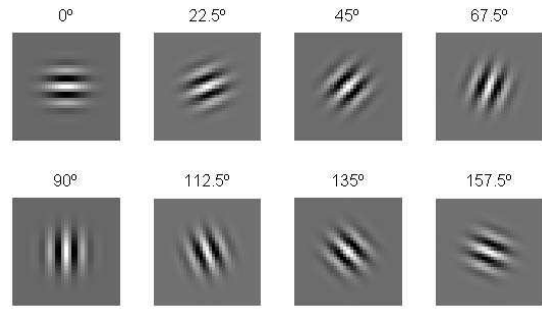


Figure 5: Gabor filters with eight orientations for texture extraction.

The matching step (Daugman, 2004), computes the differences between two iris codes ($codeA$ and $codeB$) using the Hamming Distance (HD)

$$HD = \frac{\| (codeA \otimes codeB) \cap maskA \cap maskB \|}{\| maskA \cap maskB \|} \quad (7)$$

where \otimes denotes the XOR operator, while the AND operator \cap selects only the bits that have not been corrupted by eyelashes, eyelids, specular reflections, etc, and $\| \cdot \|$ represents the norm of the vectors. To take into account possible rotations between two iris images, Daugman compares the obtained HD with the one obtained using a cyclic scrolling versions of one of the images. The minimum HD gives the final matching result.

3 IMAGE DATABASES

This section describes the main features of the test images of CASIA and UBIRIS databases.

3.1 CASIA

The well-known CASIA-Chinese Academy of Sciences Institute of Automation database from Beijing, China³ has two versions:

- CASIAv1 - 756 images of 108 individuals;
- CASIAv3 - 22051 images of over 700 individuals.

On CASIAv3, the images are divided into the following categories:

- interval - digitally manipulated such that the pupil was replaced by a circular shape with uniform intensity, eliminating undesired illumination effects and artifacts such as reflection; CASIAv1 is a subset of this category;

³<http://www.sinobiometrics.com>

- lamp - images acquired under different illumination conditions, in order to produce intra-class modifications (images of a given eye taken in different sessions);
- twins - images of 100 pairs of twins.

These 320×280 , 8 bit/pixel images were acquired with an IR camera; we have used their grayscale versions.

3.2 UBIRIS

The UBIRIS database (Proença and Alexandre, 2005)⁴, was developed by the Soft Computing and Image Analysis Group of Universidade da Beira Interior, Covilhã, Portugal. This database was created to provide a set of test images with some typical perturbations such as blurred images, with reflex and eyes almost shut, being a good benchmark for systems that minimize the requirement of user cooperation. The images are captured at-a-distance and minimizing the required degree of cooperation from the users, probably even in the covert mode. Version 1 of the database (UBIRIS.v1) has 1877 images of 241 individuals, acquired in two distinct sessions:

- session 1 - acquisition in a controlled environment, with a minimum of perturbation, noise, reflection and non-uniform illumination;
- session 2 - acquisition under natural light conditions.

The images, taken with a NIKON E5700 digital RGB camera⁵, have a resolution of 200×150 pixels and a pixel-depth of 8 bit/pixel, were converted to 256-level grayscale images. Recently, a second version of the database (UBIRIS.v2) was released to be used in the Noisy Iris Challenge Evaluation challenge - Part I 11 (NICE.I). Figure 6 shows some test images: synthetic (with and without noise); real images from CASIA and UBIRIS databases. The main features of these databases are presented in table 1.

Table 1: Comparison of CASIA and UBIRIS database.

| Database | # Images | Resolution |
|----------|----------|------------------|
| CASIAv1 | 756 | 320×280 |
| CASIAv3 | 22051 | 320×280 |
| UBIRIS | 1877 | 200×150 |

⁴<http://iris.di.ubi.pt/index.html>

⁵www.nikon.com/about/news/2002/e5700.htm

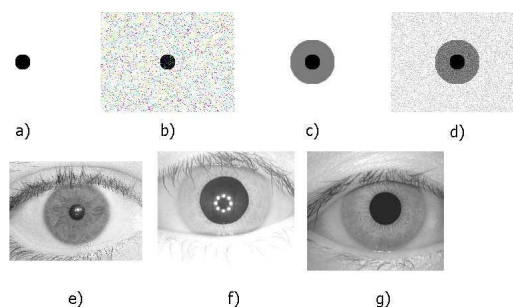


Figure 6: Test images: a) simple b) simple with noise c) pupil and iris d) pupil and iris with noise e) UBIRISv1 f) CASIAv3 g) CASIAv1.

4 MODIFICATIONS AND EXTENSIONS

4.1 Study of UBIRIS and CASIA

The accuracy of pupil and iris detection is a crucial issue in an iris recognition system. Our proposed template matching based approach estimates the pupil and the iris. In order to check for the performance of this new approach, we carried out a statistical study over UBIRIS and CASIA databases to estimate the range of pupil diameters. For both databases, we randomly collect $N=90$ images to carry out this study. For each image, we have computed the center and the radius of the pupil. Table 2 shows a statistical analysis of the pupil diameter. For both databases, the

Table 2: Study of CASIA and UBIRIS database. Statistical description of the pupil diameter (in pixels).

| Measure | CASIA | UBIRIS |
|--------------------|-------|--------|
| Mean | 86.2 | 23.7 |
| Median | 87 | 24 |
| Mode | 77 | 25 |
| Minimum | 65 | 17 |
| Maximum | 119 | 31 |
| Standard Deviation | 11.5 | 2.9 |
| Sample Variance | 132.7 | 8.3 |

increase of N over 90 does not change these statistical results. Figure 7 shows the histogram of the diameters for the CASIA database, while figure 8 does the same for UBIRIS; in this case, we see that the histogram is well approximated by a normal distribution.

4.2 PRE-PROCESSING

This section describes pre-processing techniques that we propose for UBIRIS images. The pre-processing

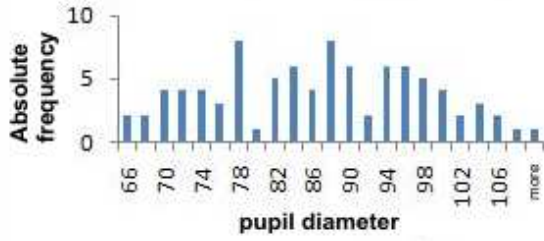


Figure 7: Histogram of pupil diameter for CASIA.

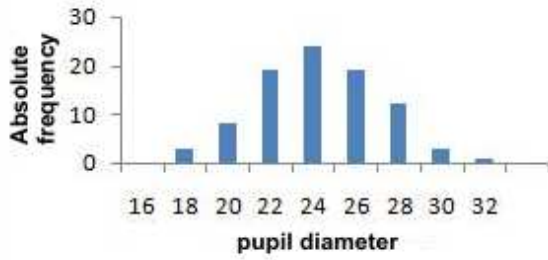


Figure 8: Histogram of pupil diameter for UBIRIS.

stage removes (or minimizes) image impairments such as noise and light reflections. Studying the images of both databases, we conclude that it is necessary to use different pre-processing strategies for each database. The pre-processing algorithms that we have devised are intended to eliminate reflections and to isolate the pupil. For this purpose, we propose 3 methods, named A, B and C. For pupil enhancement, we propose another method. These methods are necessary for UBIRIS database. The CASIAv1 images are already pre-processed.

4.2.1 Method A

Taken a histogram analysis, from a set of 21 images, we conclude that the pupil has low intensity values, corresponding to 7% to 10% of the image. This way, we found the range of intensities between the pupil and the iris. From this range of intensities, we compute a threshold between the pupil and the iris, as depicted by T in figure 9. The actions taken by method A for reflection removal are as follows.

Method A for reflection removal

Input: I_{in} - input image, with 256 gray-levels
Output: I_{out} - image without reflections on the pupil

1. From the histogram of I_{in} compute a threshold T (as in figure 9) to locate the pupil pixels.

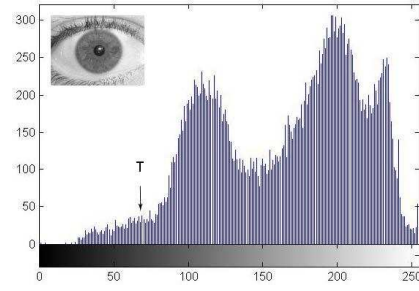


Figure 9: Typical histogram of an iris image.

2. Set the pupil pixels (gray level below T) to zero.
 3. Locate and isolate the reflection area, with an edge detector and a filling morphologic filter (Lim, 1990).
 4. $I_{out} \leftarrow$ image with the reflection area pixels set to zero.
-

Figure 10 illustrates the application of method A: on stage a) we see a white reflection on the pupil; this reflection is removed on stage d).

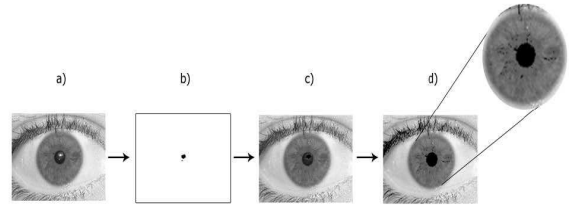


Figure 10: Reflex removal by method A: a) original image; b) isolated reflection c) image without reflection d) image with an uniform pupil.

4.2.2 Method B

This method uses a threshold to set to a certain value the pixels on a given Region of Interest (ROI).

Method B for reflection removal

Input: I_{in} - input image, with 256 gray-levels
 X, Y - upper-left corner of ROI
 W, H - width and height of ROI
 T - threshold for comparison

Output: I_{out} - image without reflections on the pupil

1. Over I_{in} locate the set of pixels below T .
2. Isolate this set of pixels, to form the ROI.
3. Horizontally, make top-down scan of the ROI and for each line, replace each pixel in the line by the average of the pixels at both ends of that line.

4. $I_{out} \leftarrow$ image with the ROI pixels set to this average value.

4.2.3 Method C

This third method uses morphologic filters (Lim, 1990) to fill areas with undesired effects, such as a white circumference with a black spot. In this situation, the morphologic filter fills completely the white circumference. This filter is applied on the negative version of the image and after processing, the image is put back to its original domain.

Method C for reflection removal

Input: I_{in} - input image, with 256 gray-levels

Output: I_{out} - image without reflections on the pupil

1. $\tilde{I}_{in} \leftarrow$ negative version of I_{in} (Lim, 1990).
 2. $\tilde{I}_p \leftarrow$ output of the morphologic filling filter on \tilde{I}_{in} .
 3. $I_{out} \leftarrow$ negative version of \tilde{I}_p .
-

Figure 11 shows the results obtained by this method; we can see clearly the removal of the white reflection. Among these three methods, this one is the fastest; it takes (on average) about 40 ms to run on a UBIRIS image.

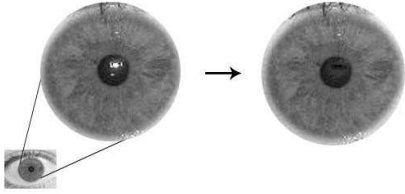


Figure 11: Illustration of reflex removal by method C.

4.2.4 Pupil isolation

After reflection removal, we introduced a pupil enhancement algorithm to obtain better results in the segmentation phase. This way, we isolate the pupil from the rest of the image. The algorithm for pupil isolation is divided into four stages: **enhancement and smooth** - apply a reflex removal method and a gaussian filter to smooth the image; **detection** - edge and contour detection of the pupil, producing a binary image; **isolation** - remove the contours outside a specific area, isolating the pixels along the pupil; **dilation and filling** - dilate the image and fill the points across the pupil.

Pupil isolation

Input: I_{in} - input image, with 256 gray-levels

σ - standard deviation for the gaussian filter

T - minimum number of pupil pixels

Output: I_{out} - binary image with an isolated pupil

1. Remove reflections (methods A, B or C) on I_{in} .
 2. Apply a gaussian filter G_σ to smooth the image.
 3. Apply the Canny Edge (Lim, 1990) detector for pupil and iris detection; retain only the pupil area.
 4. While the number of white pixels is below T , dilate the detected contours.
 5. $I_{out} \leftarrow$ output of the filling morphologic filter.
-

4.3 SEGMENTATION

The segmentation phase is of crucial importance, because without a proper segmentation it is impossible to perform recognition. We propose the following methods for segmentation: versions of the integro-differential operator; template matching. For the first we propose the following options: **version 1** - simplified version of (2) without the gaussian smoothing function; **version 2** - finite difference approximation to the derivative and interchanging the order of convolution and integration as in (Daugman, 1993); **version 3** - the operator as in (2). In order to speed up the performance of the operator we have considered a small range of angles to compute the contour integral: 180° ($\theta \in [-\pi/4, \pi/4] \cup [3\pi/4, 5\pi/4]$).

For UBIRIS, we devised a new strategy for the segmentation phase, based on a template matching approach. We propose to automatically segment the image using cross-correlation between the iris images and several templates and finding the maximums of this operation. Template matching is an extensively used technique in image processing (Lim, 1990). Since the iris and pupil region have a circle format (or approximate) this technique is considered very suitable, being only necessary to use circle templates with different sizes (it not necessary to take into account rotations of the templates). To cope with the range of diameters, we have used several versions of the templates. Supported by the study presented on section 4.1, we considered a range of diameters that covers 90% of the diameters displayed in figure 8, to narrow the number of templates. This way, we have chosen the set of diameters $D = \{20, 22, 24, 26, 28, 30\}$; four of these templates are depicted in figure 12. The difference between two consecutive templates is two pixels. We have found that is not necessary to consider the entire

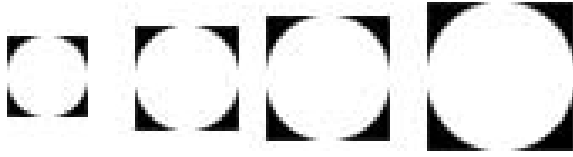


Figure 12: Templates used for the proposed template matching-based segmentation stage on UBIRIS database.

set of integers, in order to have an accurate estimation of the diameter (this way, we decrease the number of comparisons to half). For the CASIA database, we proceed in a similar fashion obtaining diameters $D = \{70, 72, 74, \dots, 124\}$. The cross-correlation based template matching technique has an efficient implementation using FFT (Fast Fourier Transform) and its inverse (Lim, 1990).

5 EXPERIMENTAL RESULTS

This section reports our experimental results obtained with our variants and modifications to Daugman approach, obtained with our C# application. Figure 13 shows a screen shot of the developed application, with the following functionalities: **enrollment** - register an individual in the system; **authentication** - verify the identity of an already registered user; **identification** - search for an individual. Regarding the

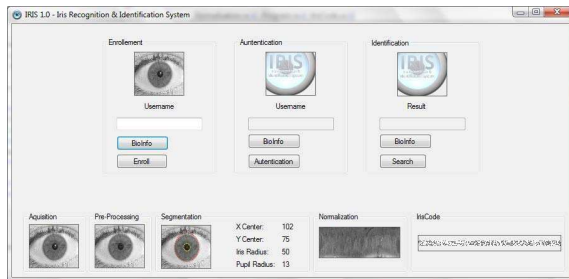


Figure 13: Developed application.

pre-processing stage, we have found that the reflection removal methods A, B and C presented in section 4.2 attained good similar results as can be seen by figures 10 and 11. The pupil enhancement algorithm also got good results improving the segmentation stage.

5.1 Segmentation

For the segmentation phase of Daugman's algorithm, the variants described in section 4.3, regarding the

integro-differential operator and template matching were tested.

5.1.1 Integro-differential operator

We have found that the (fast) first version of the integro-differential operator, obtained satisfactory results only for synthetic images. The second version performed a little better, but the results still were unsatisfactory. Table 3 shows the percentage of success in the detection of the diameter and center of pupil and iris, for the third version of the operator (the slowest and most accurate version). On table 3, the

Table 3: Integro-differential operator - version 3. From CASIAv3, the 756 images were randomly selected.

| Database | Success |
|------------------------|---------|
| UBIRISv1 (1877 images) | 95.7 % |
| CASIAv1 (756 images) | 98.4 % |
| CASIAv3 (756 images) | 94 % |

worst results for CASIAv3 and UBIRIS are justified by the fact that these images contain reflections. The already pre-processed CASIAv1 images, as stated in section 3.1, are easier to segment, justifying better results.

5.1.2 Template Matching

Replacing the integro-differential operator by the template matching technique to perform the segmentation, we get the results displayed in table 4. Comparing the test results of tables 4 and 3, we have

Table 4: Template Matching for segmentation.

| Database | Success |
|------------------------|---------|
| UBIRISv1 (1877 images) | 96.3 % |
| CASIAv1 (756 images) | 98.5 % |
| CASIAv3 (756 images) | 98.8 % |

a better results and lower processing time. In our tests, on both databases the template matching approach runs about 7 to 10 times faster than the third version of the integro-differential operator. The template matching segmentation takes 0.1 and 1.5 seconds for UBIRIS and CASIA, respectively. This (big) difference is due to the larger resolution CASIA images; we have to use a larger number of templates (4 times as for UBIRIS). Finally, considering the sequence template matching followed by the integro-differential operator we run the same tests, obtaining the results on table 5. Comparing tables 5 and 4, we conclude that this combination has a very small gain, only for CASIAv1 and has larger computation time

Table 5: Template Matching followed by integro-differential operator for segmentation.

| Database | Success |
|------------------------|---------|
| UBIRISv1 (1877 images) | 96.3 % |
| CASIAv1 (756 images) | 98.7 % |
| CASIAv3 (756 images) | 98.8 % |

than the previous approach. This way, it is preferable to use solely the template matching technique.

5.2 Recognition rate

Using Gabor filters with eight orientations (see figure 5) and four frequencies, our implementation got a recognition rate of 87.2% and 88%, for UBIRISv1 and CASIAv1, respectively. This recognition rate can be improved; it is known that it is possible to achieve higher recognition rate with Daugman's method on CASIAv1, using a larger IrisCode (Masek, 2003). Our main goal in this work was to show that when we do not have infra-red already pre-processed (CASIAv1-like) images: the reflection removal pre-processing stage is necessary; sometimes pupil enhancement methods are also necessary; the segmentation stage can be performed much faster with an efficient FFT-based template matching approach.

6 CONCLUSIONS

We addressed the problem of iris recognition, by modifying and extending the well-known Daugman's method. We have developed a C# application and evaluated its performance on the public domain UBIRIS and CASIA databases. The study that was carried out over these databases allowed us to propose essentially two new ideas for: reflex removal; enhancement and isolation of the pupil and iris. For the reflex removal problem, we have proposed 3 different methods. The enhancement and isolation of the pupil, based on morphologic filters, obtained good results for both databases. It is important to stress that this pre-processing algorithms depend on the image database. Regarding the segmentation stage, we replaced the proposed integro-differential operator by an equally accurate and faster cross-correlation template matching criterion, which has an efficient implementation using the FFT and its inverse. This way, we have improved the segmentation stage, because the template matching algorithm is more tolerant to noisy images, when compared to the integro-differential operator and runs faster. As future work we intend to tune the algorithm for the noisy UBIRIS database.

REFERENCES

- Arvacheh, E. M. (2006). A study of segmentation and normalization for iris recognition systems. Master's thesis, University of Waterloo.
- Boles, W. (1997). A security system based on iris identification using wavelet transform. In L.C.Jain, editor, *First Int Conf on Knowledge-Based Intelligent Electronic Systems*, pages 533–541, Adelaide, Australia.
- Daugman, J. (1993). High confidence visual recognition of persons by a test of statistical independence. *IEEE Transactions on Pattern Analysis and Machine Intelligence*, 25(11):1148–1161.
- Daugman, J. (2004). How iris recognition works. *IEEE Transactions on Circuits and Systems for Video Technology*, 14(1):21–30.
- Greco, J., Kallenborn, D., and Nechyba, M. C. (2004). Statistical pattern recognition of the iris. In *17th annual Florida Conference on the Recent Advances in Robotics (FCRAR)*.
- Jain, A. K., Ross, A., and Prabhakar, S. (2004). An introduction to biometric recognition. *IEEE Transactions on Circuits and Systems for Video Technology*, 14(1).
- J.Huang, Y.Wang, T.Tan, and J.Cui (2004). A new iris segmentation method for recognition. In *17th Int Conf on Pattern Recognition (ICPR'04)*.
- Joung, B. J., Kim, J. O., Chung, C. H., Lee, K. S., Yim, W. Y., and Lee, S. H. (2005). On improvement for normalizing iris region for a ubiquitous computing. *Computational Science and Its Applications ICCSA 2005*, pages 1213–1219.
- Lim, J. (1990). *Two-dimensional Signal and Image Processing*. Prentice Hall.
- Maltoni, D., Maio, D., Jain, A. K., and Prabhakar, S. (2005). *Handbook of Fingerprint Recognition*. Springer, 1th edition.
- Masek, L. (2003). Recognition of human iris patterns for biometric identification. Master's thesis, University of Western Australia.
- Proença, H. (2007). *Towards Non-Cooperative Biometric Iris Recognition*. PhD thesis, Universidade da Beira Interior.
- Proença, H. and Alexandre, L. A. (2005). UBIRIS: a noisy iris image database. *Lecture Notes in Computer Science ICIAP 2005 - 13th International Conference on Image Analysis and Processing*, 1:970–977.
- Vatsa, M., Singh, R., and Gupta, P. (2004). Comparison of iris recognition algorithms. In *Proceedings of International Conference on Intelligent Sensing and Information Processing*, pages 354–358.
- Wildes, R. (1997). Iris recognition: an emerging biometric technology. *Proceedings of the IEEE*, 85(9):1348–1363.
- Yao, P., Li, J., Ye, X., Zhuang, Z., and Li, B. (2006). Analysis and improvement of an iris identification algorithm. In *18th International Conference on Pattern Recognition (ICPR'06)*.